Using Mutability Landscapes To Guide Enzyme Thermostabilization

Chao Guo,[a] Yan Ni,[a, d] Lieuwe Biewenga,[a, d] Tjaard Pijning,[b] Andy-Mark W. H. Thunnissen,[c] and Gerrit J. Poelarends*[a]

Thermostabilizing enzymes while retaining their activity and enantioselectivity for applied biocatalysis is an important topic in protein engineering. Rational and computational design strategies as well as directed evolution have been used successfully to thermostabilize enzymes. Herein, we describe an alternative mutability-landscape approach that identified three single mutations (R11Y, R11I and A33D) within the enzyme 4-oxalocrotonate tautomerase (4-OT), which has potential as a biocatalyst for pharmaceutical synthesis, that gave rise to significant increases in apparent melting temperature T_m (up to 20 °C) and in half-life at 80 °C (up to 111-fold). Introduction of these beneficial mutations in an enantioselective but thermolabile 4-OT variant (M45Y/F50A) afforded improved triple-mutant enzyme variants showing an up to 39 °C increase in T_m value, with no reduction in catalytic activity or enantioselectivity. This study illustrates the power of mutability-landscape-guided protein engineering for thermostabilizing enzymes.

Introduction

Enzyme thermostability is an attractive feature for industrial biocatalysis because it allows for the use of higher process temperatures, which might be helpful to achieve higher reaction rates, improved substrate solubility, better mixing because of decreased viscosity of the solvent, and inhibition of microbial growth.[1] Thermostable enzymes are often also more stable towards high substrate, product and cosolvent concentrations, as well as other destabilizing reaction conditions.[1c,2] Moreover, in a laboratory setting, thermostable enzymes are the preferred starting points for generating highly active biocatalysts by directed evolution because the evolution of activity often comes at the cost of stability.[3] Given that most enzymes isolated from mesophilic microorganisms show relatively low stability, the thermostabilization of enzymes has become an increasingly important topic in protein engineering.[1d,3d,4]

Various protein engineering strategies for improving enzyme stability have been reported, including error-prone PCR-based directed evolution, focused mutagenesis based on crystallographic B-factors, rational design based on the stabilization of flexible (loop) regions or improved interactions between subunits, ancestral sequence reconstruction, and advanced computational design strategies.[2b,3a–d,5] Another interesting concept in enzyme engineering is the generation of large-scale mutational data in order to chart protein mutability landscapes, which is a powerful tool that can be used to identify functional "hotspots" at any place in the amino acid sequence of an enzyme.[6] These "hotspot" positions can be used as targets for combinatorial mutagenesis to yield enzymes with improved properties. We have previously used this mutability landscape approach to engineer 4-oxalocrotonate tautomerase (4-OT), an enzyme that utilizes an N-terminal proline to promiscuously catalyze synthetically useful asymmetric carbonyl transformations via enamine and iminium ion intermediates,[7] towards improved Michael-type addition, aldol condensation and peroxygenase activity, as well as enhanced stereoselectivity and cosolvent stability.[6a,7c,8]

In this study, we explored the use of mutability-landscape-guided protein engineering for improving the thermostability of 4-OT. To this end, we used a collection of nearly all single-mutant variants of 4-OT to investigate the effect of each mutation on the ability of the enzyme to retain its activity at elevated temperatures. Three mutations, A33D, R11Y and R11I, resulted in enzyme variants with remarkable increases in apparent melting temperature T_m and in half-life at 80 °C. Introduction of one of these beneficial mutations in a previously engineered enantioselective but thermolabile 4-OT variant (M45Y/F50A) afforded an improved enzyme variant (R11I/M45Y/

[a] C. Guo, Y. Ni, L. Biewenga, Prof. Dr. G. J. Poelarends
Department of Chemical and Pharmaceutical Biology
Groningen Research Institute of Pharmacy, University of Groningen
Antonius Deusinglaan 1, 9713 AV Groningen (The Netherlands)
E-mail: g.j.poelarends@rug.nl
[b] Dr. T. Pijning
Structural Biology Group,
Groningen Institute of Biomolecular Sciences and Biotechnology
University of Groningen
Nijenborgh 7, 9747 AG Groningen (The Netherlands)
[c] Dr. A.-M. W. H. Thunnissen
Molecular Enzymology Group
Groningen Institute of Biomolecular Sciences and Biotechnology
University of Groningen, Nijenborgh 4, 9747 AG Groningen (The Netherlands)
[d] Y. Ni, L. Biewenga
Present address: Department of Biomedical Engineering
Eindhoven University of Technology
5600 MB Eindhoven (The Netherlands)

Supporting information for this article is available on the WWW under https://doi.org/10.1002/cbic.202000442

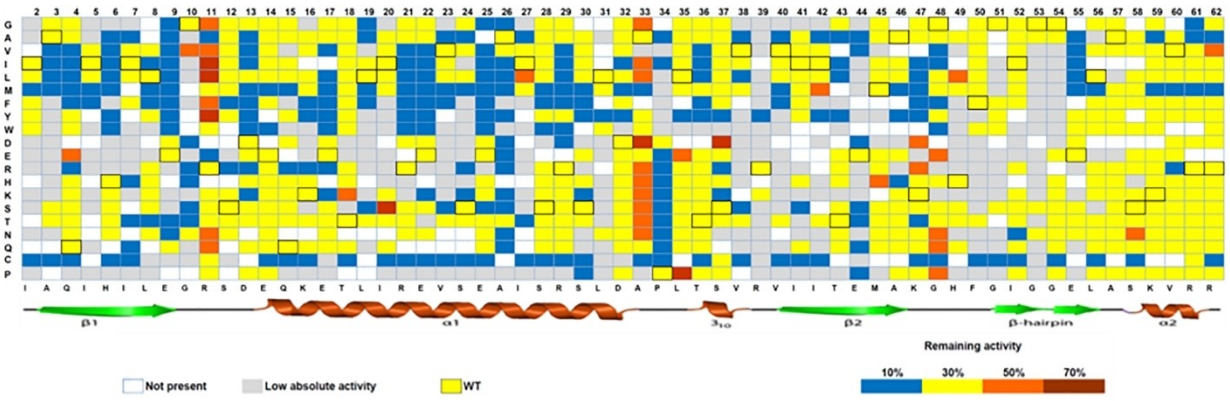

Figure 1. Thermostability mutability landscape of 4-OT. The horizontal axis of the data matrix represents the residue position of 4-OT, starting with Ile2 and ending with Arg62. The vertical axis represents all 20 canonical amino acids. For clarity, the wild-type amino acid at each position is indicated with a bold square. White squares indicate that this mutant is not present in the collection. The color of the other squares indicates the residual "Michaelase" activity of 4-OT mutants after 1 h of incubation at 80 °C compared to that after 1 h of incubation at 25 °C. Grey boxes indicate that the "Michaelase" activity was too low to determine the remaining activity. A "hotspot" position is defined as an amino acid residue position at which several single mutations result in enzyme variants that show high (> 50%) remaining activity at the elevated temperature.

F50A) showing a 39 °C increase in T_m value, with no reduction in activity or enantioselectivity.

Results

In order to identify "hotspot" positions of 4-OT at which mutations increase the thermostability of the enzyme, a defined collection of 1040 single-mutant variants of 4-OT was screened using cell-free extracts (CFEs) prepared from cultures each expressing a different 4-OT mutant.[6a] The single-mutant variants were incubated for 1 h at 25 or 80 °C, and the remaining "Michaelase" activity (using acetaldehyde and *trans*-β-nitrostyrene as the substrates) after incubation at 80 °C, compared to that after incubation at 25 °C, was graphically represented in a mutability landscape for thermostability (Figure 1). Analysis of the mutability landscape revealed two "hotspot" positions, Arg11 and Ala33, at which single mutations resulted in enzyme variants that showed more than 50% remaining activity at the elevated temperature. Interestingly, mutant A33D, which has previously been shown to possess high enantioselectivity and increased "Michaelase" activity,[6a] as well as improved stability towards high ethanol concentrations,[8c] appears to also have enhanced thermostability.

In an attempt to further increase the thermostability of 4-OT, a combinatorial saturation mutagenesis library at "hotspot" positions Arg11 and Ala33 was constructed using wild-type 4-OT as the template. However, we could not produce enough soluble 4-OT protein in cultures grown in 96-well plates for thermostability assessments. Therefore, as an alternative strategy, the mutation A33D was combined with mutation R11I, R11Y, R11Q, R11L or R11F. These single mutations at position 11 were selected because they resulted in enzyme variants that showed more than 50% remaining activity at 80 °C (Figure 1). Appropriate amounts of soluble protein could be produced and purified from larger cell cultures grown in 5 L flasks with rigorous shaking. However, the double mutants showed lower activity and a decreased apparent melting temperature T_m compared to the best single mutants (Table S1 in the Supporting Information); this indicates that combining these mutations at positions 11 and 33 does not result in a further increase in the thermostability of 4-OT.

The three single-mutant 4-OT variants A33D, R11I and R11Y were purified and investigated in more detail with regard to their stability at elevated temperatures. Upon incubation at 80 °C, the wild-type enzyme was inactivated within 60 min, whereas the mutant enzyme A33D retained ~40% activity after 360 minutes of incubation (Figure 2A). Remarkably, the mutant enzymes R11I and R11Y retained ~90% activity after 360 minutes of incubation at 80 °C (Figure 2A), and only after incubation at 100 °C for 240 min we could observe significant inactivation of these 4-OT variants (Figure 2B). The half-life ($t_{1/2}$) values of A33D, R11Y and R11I at 80 °C were 285, 1260 and 1980 min, which were about 16, 71 and 111 times higher than that of the wild-type enzyme, respectively (Table 1).

Next, the enzyme thermostability was evaluated by determining the T_{50}^{120} (Figure 2C), the temperature at which the enzyme lost 50% of its activity after 120 minutes of incubation. To this end, the remaining activities of wild-type 4-OT and the 4-OT mutants were assessed after incubating each enzyme at

Table 1. Properties of wild-type 4-OT and 4-OT mutants.[a]

4-OT	$t_{1/2}$ [min][b]	T_{50}^{120} [°C][c]	T_m [°C]
WT	17.8 ± 1.5	68.7 ± 1.3	73.8 ± 0.1
A33D	285 ± 36	79.8 ± 1.4	77.9 ± 0.1
R11I	1980 ± 52	95.5 ± 0.5	94.0 ± 0.1
R11Y	1260 ± 73	88.4 ± 2.2	92.0 ± 0.2

[a] Values represent the mean of three independent sets of experiments. [b] $t_{1/2}$ represents the half-life at 80 °C. [c] Temperature at which the enzyme lost 50% activity after incubation for 120 min.

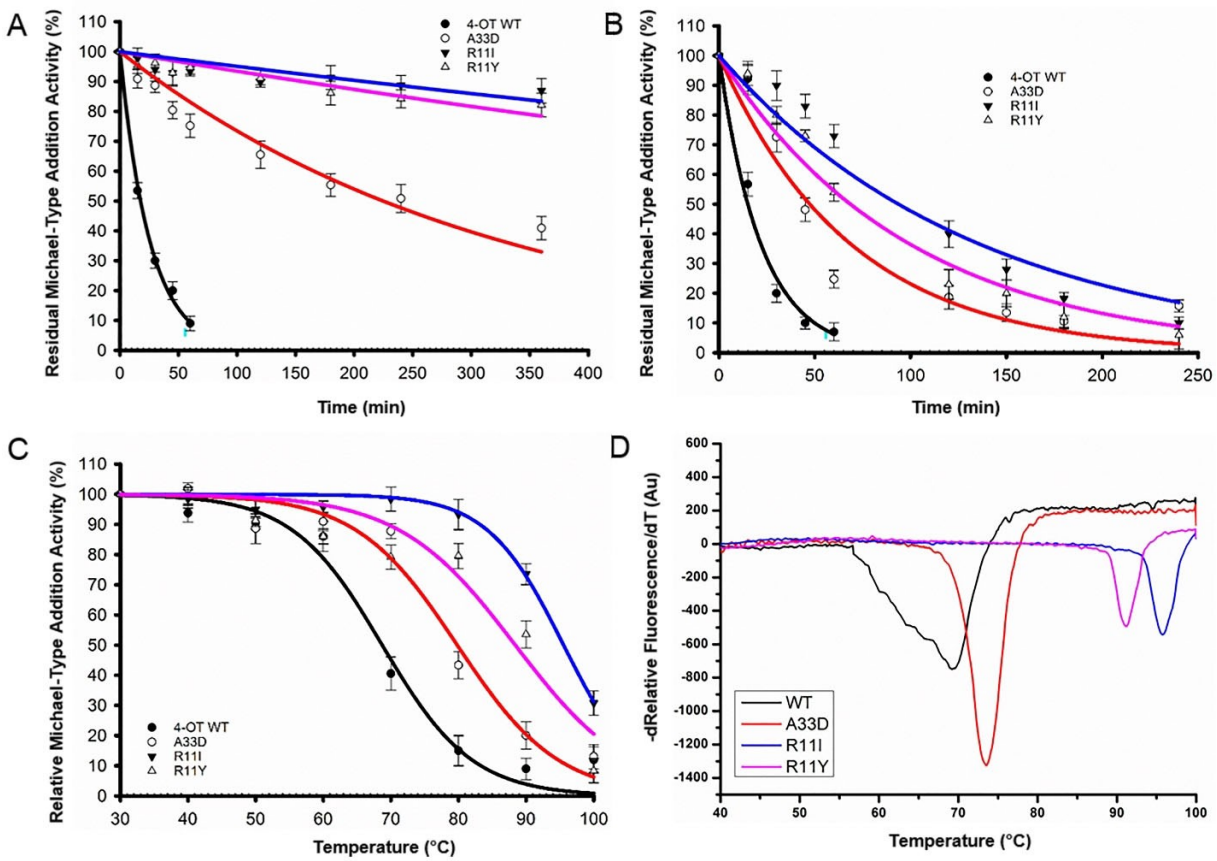

Figure 2. Thermostability assessment of wild-type 4-OT and the three single-mutant 4-OT variants. A) Activity decay at 80 °C. B) Activity decay at 100 °C. C) Determination of T_{50}^{120} values. D) The first derivatives of each melting curve where each minimum indicates the apparent melting temperature T_m for wild-type 4-OT and the three 4-OT mutants. The T_m values reported in the text and Table 1 were obtained by fitting the original melting curves.

temperatures from 30 to 100 °C. Whereas no significant differences in remaining activity were observed with treatment below 50 °C, incubation at temperatures above 60 °C showed large variances in remaining activity for the different enzymes (Figure 2C). For example, the remaining activity of wild-type 4-OT was only 40% after treatment for 120 min at 70 °C, while the single-mutant 4-OT variant R11I retained ~100% of its activity after the same treatment. The curves shown in Figure 2C gave T_{50}^{120} values of 68.7 °C for wild-type, 79.8 °C for mutant A33D, 88 °C for mutant R11Y, and 95.5 °C for mutant R11I. Finally, the apparent melting temperature T_m of each enzyme was measured by differential scanning fluorimetry (Figure 2D). The resulting melting curves gave T_m values of 73.8 °C for wild-type, 77.9 °C for A33D, 92 °C for R11Y and 94 °C for R11I (Table 1).

Using acetaldehyde and *trans*-β-nitrostyrene as the substrates, we determined apparent kinetic parameters for wild-type 4-OT and the single-mutant 4-OT variants (Table 2). Whereas mutant A33D showed a 2.2-fold increase in k_{cat}, mutants R11I and R11Y showed a 1.6-fold and 3.5-fold, respectively, decrease in k_{cat} compared to that of the wild-type enzyme (Table 2). Notably, the mutations only have a minor effect on the stereoselectivity of 4-OT, with mutant A33D showing nearly perfect enantioselectivity (Table 2, Figure S1).

Table 2. Apparent kinetic parameters for the Michael-type addition of acetaldehyde to *trans*-β-nitrostyrene catalyzed by wild-type 4-OT and single-mutant 4-OT variants.[a]

4-OT	K_m [mM]	k_{cat} [s^{-1}] $\times 10^3$	k_{cat}/K_m [$s^{-1} M^{-1}$]	Conf.[b]	*er*
wild type	0.38 ± 0.067	23.2 ± 1.4	61.0 ± 4.5	*S*	97:3
A33D	0.36 ± 0.028	50.6 ± 1.3	140.6 ± 15.7	*S*	>99:1
R11I	0.46 ± 0.039	14.0 ± 0.4	30.5 ± 3.7	*S*	95:5
R11Y	0.09 ± 0.005	6.5 ± 0.1	73.0 ± 5.3	*S*	98:2

[a] Apparent kinetic parameters were determined by using various *trans*-β-nitrostyrene concentrations and 100 mM acetaldehyde at 25 °C and pH 7.3. The values shown indicate mean ± standard deviation from three parallel experiments. [b] Determination of absolute configuration was based on chiral GC and previously reported chiral GC data with authentic standards (Figure S1).[6a,8c]

Next, we investigated whether the identified single mutations that are beneficial for thermostability can confer high thermostability to 4-OT variant M45Y/F50A. This double-mutant variant was chosen because it is highly enantioselective, produces the pharmaceutically relevant *R* enantiomer of the γ-nitroaldehyde product, and is thermolabile (Table S1).[6a] To this end, three new triple mutants were generated by the introduction of mutation R11I, R11Y or A33D into 4-OT M45Y/

F50A as the starting template. Differential scanning fluorimetry experiments showed that all three triple mutants are significantly more thermostable than parental mutant 4-OT M45Y/F50A, with T_m values of 84 °C for A33D/M45Y/F50A, 92 °C for R11Y/M45Y/F50A, and 96 °C for R11I/M45Y/F50A (Table S1). Activity assays showed that A33D/M45Y/F50A (2.7-fold), R11Y/M45Y/F50A (1.7-fold), and R11I/M45Y/F50A (2.4-fold) have even slightly increased Michael-type addition activity compared to M45Y/F50A, while retaining the high enantioselectivity towards the desired *R* enantiomer of the product (Table S1, Figure S2).

Discussion

In this study, a mutability landscape approach was applied to discover two "hotspot" positions within the enzyme 4-OT, Arg11 and Ala33, at which single mutations resulted in enzyme variants that showed a significant increase in apparent melting temperature T_m (up to 20 °C) and in half-life at 80 °C (up to 111-fold). Although there was no positive effect of combining the mutations at positions 11 and 33 on the thermostability of 4-OT, we used the information from the mutability landscape to further engineer a previously constructed enantioselective 4-OT variant (M45Y/F50A) that exhibits relatively poor thermostability.[6a] The introduction of the identified beneficial mutations (R11Y, R11I and A33D) in 4-OT variant M45Y/F50A afforded improved triple-mutant enzyme variants, with the best enzyme (R11I/M45Y/F50A) showing a 39 °C increase in T_m value with no reduction in catalytic activity or enantioselectivity. These results further demonstrate the power of mutability-landscape-guided protein engineering for improving enzyme properties.[6b]

Interestingly, residue Ala33 was previously identified as a "hotspot" position at which mutations are beneficial for catalysis in high concentrations of the cosolvent ethanol.[8c] Particularly, the 4-OT variant A33D not only showed improved ethanol tolerance,[8c] but also enhanced Michael-type addition activity and enantioselectivity.[6a] This single point mutation thus has a beneficial effect on the activity, stereoselectivity, solvent stability and thermostability of 4-OT. Such functional plasticity is also observed for mutations at position Arg11, with 4-OT variants R11I and R11Y now demonstrated to be extremely thermostable. Although Arg11 is essential for the native tautomerase activity of 4-OT, most mutations at this position have no effect on the Michael-type addition activity of the enzyme.[6a] Because of their positive effects on activity and stability, these single mutations at positions Arg11 and Ala33 were used in combination with the enantioselective 4-OT variant M45Y/F50A to create active, enantioselective and thermostable biocatalysts. Other identified beneficial mutations for thermostability, like I20S, L35P and S37D (Figure 1), have not been tested in combination with variant M45Y/F50A because previously constructed mutability landscapes showed that these single mutations have a negative effect on the Michael-type addition activity of 4-OT.[6a] Hence, the construction of mutability landscapes for multiple properties of one enzyme provides the exciting opportunity to select mutations that are beneficial either for one or for several of these properties.[6b]

Inspection of the crystal structure of wild-type 4-OT does not provide an obvious explanation for the improved thermostability caused by mutations at positions Arg11 and Ala33, thus illustrating the effectiveness of mutability-landscape navigation to identify functional "hotspot" positions. By determining crystal structures of 4-OT variants A33D and R11I, we aim to explain the multifunctional effects of these interesting point mutations. The large amount of mutational data generated within this study may be used as a unique training set to generate improved mutation prediction models for enhancing enzyme thermostability. More accurate computational predictions necessitates less experimental testing of enzyme mutants, accelerating enzyme thermostabilization.

Experimental Section

Production of cell-free extracts: The thermostability of all members of the 4-OT mutant collection was determined using CFEs of *Escherichia coli* BL21(DE3) cultures each expressing a different 4-OT mutant. These CFEs were prepared according to a reported procedure.[6a,7c] Concisely, 1.25 mL of LB medium supplemented with 100 μg/mL ampicillin and 100 μM isopropyl-β-D-1-thiogalactopyranoside (IPTG) was inoculated from a glycerol stock of the corresponding mutant and the culture was grown overnight at 37 °C in a 96-deep-well plate (Greiner Bio-one, 96 well Masterblock®). Each mutant was inoculated in duplicate. The deep-well plates were sealed with sterile, gas-permeable seals (Greiner Bio-one, BREATHseal™) and incubated overnight at 37 °C with shaking at 200 rpm. The cells from the overnight cultures were harvested by centrifugation (2232*g* for 30 min at 4 °C) and lysed with 300 μL of Bugbuster (Novagen), supplemented with 25 U/mL benzonase, for 40 min. After centrifugation (2916*g* for 60 min at 4 °C), the obtained CFE was used for the activity assay.

Construction of the mutability landscape of 4-OT for thermostability: The CFEs prepared from cells producing 4-OT single-mutant variants were transferred into 96-well PCR plates (semi-skirted, ThermoFisher Scientific), after which the plates were sealed with thermoresistance mats (Thermo Scientific VersiCap™ Mats), resulting in plates with 50 μL CFE in each well. The plates were then incubated at 25 °C (control plate) or 80 °C for 1 h in a PCR thermocycler. The plates were then placed on ice for 20 min, followed by centrifugation at 4000 rpm for 30 min, after which 20 μL supernatant of each CFE was transferred into a 96-well microtiter plate (MTP; UV-star μclear, Greiner Bio-one) and used for measuring residual enzyme activity.

The reaction mixture (100 μL final volume) used to monitor the 4-OT-catalyzed Michael-type addition of acetaldehyde to *trans*-β-nitrostyrene consisted of the following: CFE (20% *v/v*), acetaldehyde (50 mM), *trans*-β-nitrostyrene (0.5 mM) and ethanol (5% *v/v*) in 20 mM NaH_2PO_4 buffer (pH 7.3). First, the appropriate amounts of CFE and buffer were added to each well of the MTP, using a Packard Multiprobe® II HT EX 8 tip robotic liquid-handling system. The assay was then initiated by adding 5 μL of a stock solution of *trans*-β-nitrostyrene (10 mM in ethanol) and 5 μL of a stock solution of acetaldehyde (1 M in 20 mM NaH_2PO_4 buffer, pH 7.3) to each well of the MTP. The MTPs were sealed with UV-transparent plate seals (VIEWseal™, Greiner Bio-one) to minimalize evaporation of reaction components. To ensure proper mixing of the reagents, the plate was shaken (30 s at 500 rpm) immediately after all reaction components were added. Reaction progress was monitored in a

SPECTROstar Omega plate reader (BMG Labtech, Isogen Life Science, de Meern, NL) by following the depletion in absorbance at 320 nm, corresponding to the concentration of *trans*-β-nitrostyrene, for 80 min with a 60 s data interval. The slope of the linear part of the curve was determined for each reaction. The remaining enzyme activity was determined by dividing the slope of the reaction at 80 °C by the slope of the reaction at 25 °C.

4-OT purification: The 4-OT enzyme, either wild-type or mutant, was produced in *E. coli* BL21(DE3) by using the pET20b(+) expression system. LB medium (5 mL) containing ampicillin (100 μg/mL) was inoculated with cells from a glycerol stock of *E. coli* BL21(DE3) containing the appropriate expression vector by using a sterile loop. After overnight growth at 37 °C, this culture was used to inoculate fresh LB/ampicillin medium (1 L) in a 3 L Erlenmeyer flask. Cultures were grown overnight at 37 °C with vigorous shaking. Cells were harvested by centrifugation and stored at −20 °C. The purification of 4-OT variants (constructed using QuikChange technology) was based on previously reported procedures.[6a,7a] All purified proteins were >90% pure as assessed by SDS-PAGE (Figure S3). 4-OT variants were analyzed by electron spray ionization mass spectrometry (ESI-MS) to confirm that the proteins had been processed correctly and the initiating methionine had been removed.[6a] The purified protein was flash-frozen in liquid nitrogen and stored at −80 °C until further use.

Determination of T_{50}^{120} values: 4-OT variants (50 μL of 2 mg/mL in 20 mM NaH_2PO_4, pH 7.3) were incubated in 0.2 mL PCR tubes at temperatures ranging from 30 to 100 °C for 120 min in a thermal cycler. After this incubation, the enzymes were cooled on ice for 10 min followed by equilibration at 25 °C for 10 min. Samples were centrifuged to remove any precipitated protein. The residual enzymatic activity for the addition of acetaldehyde to *trans*-β-nitrostyrene was tested in a plate reader. The following conditions were used: 25 μL enzyme supernatant, acetaldehyde (50 mM), *trans*-β-nitrostyrene (0.5 mM) and ethanol (5% *v/v*) in 20 mM NaH_2PO_4 buffer, pH 7.3 (final volume of 100 μL). The enzymatic activities obtained after 120 min of incubation at the different temperatures were normalized to that obtained after 120 min of incubation at 30 °C. The T_{50}^{120} values were obtained by curve fitting.

Determination of $t_{1/2}$ values: The 4-OT variants (1.5 mL of 2 mg/mL in 20 mM NaH_2PO_4, pH 7.3) were incubated at 80 or 100 °C in a water bath. Aliquots (100 μL) were taken at different time points (from 0 to 360 min) and cooled immediately on ice for 10 min followed by equilibration at room temperature for 10 min. Samples were centrifuged to remove any precipitated protein. The residual enzymatic activity for the addition of acetaldehyde to *trans*-β-nitrostyrene was tested using either a V-650 or V-660 spectrophotometer from Jasco (IJsselstein, The Netherlands). The reaction mixture (0.3 mL final volume in a 1 mm cuvette) contained the following: 80 μL of enzyme supernatant, acetaldehyde (50 mM), and *trans*-β-nitrostyrene (1.5 mM, from a 30 mM stock solution in 100% ethanol) in 20 mM NaH_2PO_4 buffer (pH 7.3). The $t_{1/2}$ values were determined by curve fitting.

Differential scanning fluorimetry (DSF): The apparent melting temperature T_m of the 4-OT variants was determined by using differential scanning fluorimetry (DSF). The fluorescence change was monitored using a MyiQ real-time PCR machine (Bio-Rad, Hercules, CA, USA) with an excitation wavelength at 490 nm and an emission wavelength at 575 nm. In iQ 96-well real-time PCR plates, purified enzyme (2 mg/mL in 20 mM NaH_2PO_4, pH 6.5) was incubated with 50-fold diluted Sypro Orange dye in a total volume of 50 μL over the temperature ramp from 30 °C to 100 °C (0.1 °C per cycle, 30 s/cycle). The final fluorescence signal was the average of three independent measurements. The apparent T_m values were obtained by curve fitting.

Enzymatic synthesis: The enzyme-catalyzed Michael-type addition reactions were performed at 25 °C. The reaction mixture (2 mL final volume in a sealed container) consisted of *trans*-β-nitrostyrene (1.5 mM) and acetaldehyde (50 mM) in 20 mM NaH_2PO_4 buffer (pH 7.3). The reactions were initiated by the addition of an appropriate amount of purified enzyme (150 μg). Reaction progress was monitored by UV spectroscopy. After the reaction was completed, the reaction mixture was extracted with 400 μL ethyl acetate and the product enantiomer ratio was determined by chiral GC as reported before.[7c]

Acknowledgement

We acknowledge financial support from the Netherlands Organization of Scientific Research (VICI grant 724.016.002 and ECHO grant 713.015.003) and the European Union's Horizon 2020 Research and Innovation Programme under grant agreement No 635595 (CarbaZymes).

Conflict of Interest

The authors declare no conflict of interest.

Keywords: biocatalysis · mutability landscape · protein engineering · thermostability

[1] a) V. L. Schramm, *Annu. Rev. Biochem.* **1998**, *67*, 693–720; b) D. A. Kraut, K. S. Carroll, D. Herschlag, *Annu. Rev. Biochem.* **2003**, *72*, 517–571; c) A. Kumar, K. Dhar, S. S. Kanwar, P. K. Arora, *Biol. Proced. Online* **2016**, *18*, 2; d) F. Rigoldi, S. Donini, A. Redaelli, E. Parisini, A. Gautieri, *APL Bioeng.* **2018**, *2*, 011501.

[2] a) S. Luetz, L. Giver, J. Lalonde, *Biotechnol. Bioeng.* **2008**, *101*, 647–653; b) T. Koudelakova, R. Chaloupkova, J. Brezovsky, Z. Prokop, E. Sebestova, M. Hesseler, M. Khabiri, M. Plevaka, D. Kulik, I. K. Smatanova, P. Rezacova, R. Ettrich, U. T. Bornscheuer, J. Damborsky, *Angew. Chem. Int. Ed.* **2013**, *52*, 1959–1963.

[3] a) V. G. Eijsink, A. Bjork, S. Gaseidnes, R. Sirevag, B. Synstad, B. van den Burg, G. Vriend, *J. Biotechnol.* **2004**, *113*, 105–120; b) M. Furst, C. Martin, N. Loncar, M. W. Fraaije, *Methods Enzymol.* **2018**, *608*, 151–187; c) A. G. L. Giver, P. Freskgard, F. H. Arnold, *Proc. Natl. Acad. Sci. USA* **1998**, *95*, 12809–12813; d) H. P. Modarres, M. R. Mofrad, A. Sanati-Nezhad, *RSC Adv.* **2016**, *6*, 115252–115270.

[4] a) M. Naushad, Z. A. Alothman, A. B. Khan, M. Ali, *Int. J. Biol. Macromol.* **2012**, *51*, 555–560; b) V. G. Eijsink, S. Gaseidnes, T. V. Borchert, B. van den Burg, *Biomol. Eng.* **2005**, *22*, 21–30; c) S. Kumar, C. Tsai, R. Nussinov, *Protein Eng.* **2000**, *13*, 179–191.

[5] a) A. Korkegian, M. E. Black, D. Baker, B. L. Stoddard, *Science* **2005**, *308*, 857–860; b) Z. Wu, W. Deng, Y. Tong, Q. Liao, D. Xin, H. Yu, J. Feng, L. Tang, *Appl. Microbiol. Biotechnol.* **2017**, *101*, 3201–3211; c) A. O. Magnusson, A. Szekrenyi, H. J. Joosten, J. Finnigan, S. Charnock, W. D. Fessner, *FEBS J.* **2019**, *286*, 184–204; d) H. Yu, Y. Yan, C. Zhang, P. A. Dalby, *Sci. Rep.* **2017**, *7*, 41212; e) I. V. Korendovych, *Methods Mol. Biol.* **2018**, *1685*, 15–23; f) A. Bosshart, S. Panke, M. Bechtold, *Angew. Chem. Int. Ed.* **2013**, *52*, 9673–9676; g) Z. Sun, Q. Liu, G. Qu, Y. Feng, M. T. Reetz, *Chem. Rev.* **2019**, *119*, 1626–1665; h) Y. Xie, J. An, G. Yang, G. Wu, Y. Zhang, L. Cui, Y. Feng, *J. Biol. Chem.* **2014**, *289*, 7994–8006; i) H. J. Wijma, M. J. L. J. Fürst, D. B. Janssen, *Methods Mol. Biol.* **2018**, *1685*, 69–85; j) L. Ge, D. Li, T. Wu, L. Zhao, G. Ding, Z. Wang, W. Xiao, *J. Biotechnol.* **2018**, *275*, 17–23; k) F. S. Aalbers, M. J. L. J. Fürst, S. Rovida, M. Trajkovic, J. Rubén Gómez Castellanos, S. Bartsch, A. Vogel, A. Mattevi, M. W. Fraaije, *eLife* **2020**, *9*, e54639; l) M. T. Reetz, J. D. Carballeira, *Nat. Protoc.* **2007**, *2*, 891–903; m) Y. Gumulya, J.-M. Baek, S.-J. Wun, R. E. S. Thomson, K. L. Harris, D. J. B. Hunter, J. B. Y. H. Behrendorff, J. Kulig, S. Zheng, X. Wu, B. Wu, J. E. Stok, J. J. De Voss, G. Schenk, U. Jurva, S. Andersson, E. M. Isin, M. Bodén, L.

Guddat, E. M. J. Gillam, *Nat. Can.* **2018**, *1*, 878–888; n) H. Yu, Y. Yan, C. Zhang, P. A. Dalby, *Sci. Rep.* **2017**, *7*, 41212.

[6] a) J. Y. van der Meer, H. Poddar, B. J. Baas, Y. Miao, M. Rahimi, A. Kunzendorf, R. van Merkerk, P. G. Tepper, E. M. Geertsema, A. M. W. H. Thunnissen, W. J. Quax, G. J. Poelarends, *Nat. Commun.* **2016**, *7*, 10911; b) J. Y. van der Meer, L. Biewenga, G. J. Poelarends, *ChemBioChem* **2016**, 17, 1792–1799; c) A. Fulton, V. J. Frauenkron-Machedjou, P. Skoczinski, S. Wilhelm, L. Zhu, U. Schwaneberg, K. E. Jaeger, *ChemBioChem* **2015**, *16*, 930–936.

[7] a) E. Zandvoort, E. M. Geertsema, B. J. Baas, W. J. Quax, G. J. Poelarends, *Angew. Chem. Int. Ed.* **2012**, *51*, 1240–1243; b) H. Poddar, M. Rahimi, E. M. Geertsema, A. W. H. Thunnissen, G. J. Poelarends, *ChemBioChem* **2015**, *16*, 738–741; c) C. Guo, M. Saifuddin, T. Saravanan, M. Sharifi, G. J. Poelarends, *ACS Catal.* **2019**, *9*, 4369–4373; d) Y. Miao, M. Rahimi, E. M. Geertsema, G. J. Poelarends, *Curr. Opin. Chem. Biol.* **2015**, *25*, 115–123.

[8] a) M. Rahimi, J. Y. van der Meer, E. M. Geertsema, H. Poddar, B. J. Baas, G. J. Poelarends, *ChemBioChem* **2016**, *17*, 1225–1228; b) M. Rahimi, J. Y. van der Meer, E. M. Geertsema, G. J. Poelarends, *ChemBioChem* **2017**, *18*, 1435–1441; c) C. Guo, L. Biewenga, M. Lubberink, R. van Merkerk, G. J. Poelarends, *ChemBioChem* **2020**, *21*, 1499–1504; d) G. Xu, M. Crotti, T. Saravanan, K. M. Kataja, G. J. Poelarends, *Angew. Chem. Int. Ed.* **2020**, *59*, 10374–10378.

Manuscript received: July 6, 2020
Revised manuscript received: August 11, 2020
Accepted manuscript online: August 13, 2020
Version of record online: September 30, 2020